© Universiti Tun Hussein Onn Malaysia Publisher's Office

IJIE

Journal homepage: **http://penerbit.uthm.edu.my/ojs/index.php/ijie**

The International Journal of Integrated Engineering

Joint Source Channel Decoding Exploiting 2D Source Correlation with Parameter Estimation for Image Transmission over Rayleigh Fading Channels

Muhammad Izzat Amir Mohd Nor[1,*], Mohd Azri Mohd Izhar[1], Norulhusna Ahmad[1,], Hazilah Mad Kaidi[1]

[1] Razak Faculty of Technology and Informatics
Universiti Teknologi Malaysia, Kuala Lumpur, 54100, MALAYSIA

*Corresponding Author

DOI: https://doi.org/10.30880/ijie.2018.10.07.030
Received 26 October 2018; Accepted 25 November 2018; Available online 30 November 2018

Abstract: This paper investigates the performance of a 2- Dimensional (2D) Joint Source Channel Coding (JSCC) system assisted with parameter estimation for 2D image transmission over an Additive White Gaussian Noise (AWGN) channel and a Rayleigh fading channel. Baum-Welsh Algorithm (BWA) is employed in the proposed 2D JSCC system to estimate the source correlation statistics during channel decoding. The source correlation is then exploited during channel decoding using a Modified Bahl-Cocke-Jelinek-Raviv (BCJR) algorithm. The performance of the 2D JSCC system with the BWA-based parameter estimation technique (2D-JSCC-PET1) is evaluated via image transmission simulations. Two images, each exhibits strong and weak source correlation are considered in the evaluation by measuring the Peak Signal Noise Ratio of the decoded images at the receiver. The proposed 2D-JSCC-PET1 system is compared with various benchmark systems. Simulation results reveal that the 2D-JSCC-PET1 system outperforms the other benchmark systems (performance gain of 4.23 dB over the 2D-JSCC-PET2 system and 6.10 dB over the 2D JSCC system). The proposed system also can perform very close to the ideal 2D JSCC system relying on the assumption of perfect source correlation knowledge at the receiver that shown only 0.88 dB difference in performance gain.

Keywords: Joint Source Channel Coding, Baum-Welsh Algorithm, Markov Chain, 2-Dimensional Source Correlation, Turbo Coding.

1. Introduction

Source coding allows only necessary information to be transmitted by compressing the data while channel coding protects the data from noise and corrects the errors in the affected data at the receiver. Source and channel coding have been designed separately to obtain a reliable transmission without loss in overall performance with delay as stated by Shannon's separation theorem (Shannon,1948). However, it is not possible to achieve the ideal performance with zero delay as restriction on latency always occurs. Therefore, exploitation of the redundancy left after source encoders using channel coding/decoding would be one of the particular interest areas and hence, Joint Source and Channel Coding (JSCC) was introduced (Sayood & Borkenhagen,1991) and employed in many applications such as wireless video transmission (Huo, Wang, Maunder & Hanzo, 2013) and Hidden Markov correlation (Zhao & Garcia-Frias, 2006).

*Corresponding author: izzat_hafiez@yahoo.com

2-Dimensional (2D) source correlation was exploited during channel decoding of a JSCC system to improve the Bit Error Rate (BER) performance of (Belhadj & Boualle'gue, 2008) and (Izhar et. al., 2012). The improvement of 2D JSCC has been made into a work of (Izhar et. al., 2012) where fine-tuning method is used (Izhar et. al., 2013) and low complexity technique is considered using single parity check code (SPCCs) (Izhar et. al., 2014). A 2D image can be represented by a rectangular array of pixels where each pixel is correlated with its neighboring pixels. This correlation information can be well exploited with channel decoding to provide more protection to the image data. As a result, a high- quality image can be produced at the receiver. In other works, the effort to obtain good performance and low complexity of a JSCC system for Joint Photographic Experts Group (JPEG) 2000 image transmission was presented in (Bi & Liang, 2017).

However, all the above studies assumed that the source correlation knowledge is perfectly known at the receiver. This assumption improves the performance but it affects the reliability of the information of source correlation to be exploited at the receiver. Practically, the source correlation knowledge is unknown and hence, it needs to be estimated. Many researchers have taken up this issue and developed various parameter estimation techniques to estimate the source correlation at the receiver to ensure the correct source correlation knowledge is estimated. The 2D JSCC system with the Baum-Welsh Algorithm (BWA)-based estimation technique was proposed in (Mohd Nor et. al., 2018). The system is known as the 2D JSCC system with the Parameter Estimation 1 (2D-JSCC-PET1). The simulation results in (Mohd Nor et. al., 2018) revealed that the 2D-JSCC- PET1 system can perform very close to the ideal 2D JSCC system with perfect assumption on the availability of source correlation knowledge at the receiver.

Image transmission is commonly used as an application to demonstrate the effectiveness of coding design. In work of (Xu, H., Hua, K., & Wang, H., 2015), cooperative relayed image transmission is used under complex mobile communication channel environment, while another work has considered image transmission using a low-density-parity-check (LDPC) code over Power Line Communication (PLC) (Develi, I., Kabalci, Y., & Basturk, A., 2014). Other works used image transmission for cloud computing (Eldin, S. M. S. ,2017), Multiple-Input-Multiple-Output- Code-division multiple access (MIMO-CDMA) (Berceanu, M., Voicu, C., & Halunga, S., 2016), and a quasi random symbol interleaving technique (Azevedo, R. A., Madeiro, F., Lopes, W. T. A., & Lima, E. A. O., 2016).

In current wireless communication, a reliable transmission is a great challenge where the effect of fading always occurs. This major obstacle to wireless environment can be mitigated by employing various types of coding such as turbo codes (Hall &Wilson, 1998), JSCC using enhanced turbo codes (Aarthi, V., Kannan, S. N., & Ramanshankar, N., 2015), LDPC codes (Gautam et. al., 2014) and Reed-Solomon code (Majumder, S., & Verma, S., 2015). In this paper, we extend the work of the 2D-JSCC-PET1 system in (Mohd Nor et. al., 2018) to the application of image transmission over an Additive White Gaussian Noise (AWGN) channel and an uncorrelated Rayleigh fading channel.

The remainder of this paper is organized as follows. Section 2 describes the system model of the 2D JSCC system with parameter estimation for unknown source correlation knowledge at the receiver. Section 3 explains the system model of the 2D-JSCC-PET1 system for image transmission where two 2D images considered, one exhibits strong source correlation and the other one exhibits weak source correlation. Section 4 presents the simulation results of the 2D JSCC system and other benchmark systems for transmission over an AWGN channel. Section 5 discusses the performance of the 2D-JSCC- PET1 system for image transmission over a fading channel. Our concluding remarks are provided in conclusion section.

2. 2D JSCC system with parameter estimation

2.1 2D Source Correlation Model

The 2D correlation of a 2D source can be described by the coupling of two first-order two-state Markov chains. The current value of the source, U relies on two factors, which are the previous value in D_1 - direction (horizontal-direction), defined as U_{D_1}, and the previous value in D_2 - direction (vertical-direction), defined as, U_{D_2}. Based on the Coupled-Markov-Chain (CMC) model (Elfeki & Dekking, 2001), the transition probability matrix of the 2D source can be represented as

$$\mathbf{A} = [a_{i_1,i_2,j}] = P\{U = j \mid U_{D_1} = i_1, U_{D_2} = i_2\},$$

$$= \frac{a_{i_1,j}^{D_1}, a_{i_2,j}^{D_2}}{\sum_{k=0}^{1} a_{i_1,k}^{D_1}, a_{i_2,k}^{D_2}}, \quad i_1, i_2, j \in \{0,1\}, \tag{1}$$

where i_1, i_2 and j are the binary values generated from the previous Markov state in the horizontal-direction, the previous Markov state in the vertical-direction and the current Markov state, respectively. $a_{i_1,j}^{D_1}$ is denoted as the matrix component

of the 1D source in the horizontal-direction $\mathbf{A}^{D_1}$ and $a_{i_2,j}^{D_2}$ is the component of the matrix of the 1D source in the vertical-direction $\mathbf{A}^{D_2}$. The transition probability matrix $\mathbf{A}^{D_1}$ can be represented as

$$\mathbf{A}^{D_1} = [a_{i_1,j}^{D_1}] = \begin{bmatrix} p_0^{D_1} & 1-p_0^{D_1} \\ 1-p_1^{D_1} & p_1^{D_1} \end{bmatrix}, \quad \textbf{(2)}$$

where $p_0^{D_1}$ and $p_1^{D_1}$ are the transition probabilities of the horizontal-direction of the source that reflects to the transition from state s_0 to state s_0 and from state s_1 to state s_1 respectively. Meanwhile, the transition probability matrix $\mathbf{A}^{D_2}$ is given as

$$\mathbf{A}^{D_2} = [a_{i_2,j}^{D_2}] = \begin{bmatrix} p_0^{D_2} & 1-p_0^{D_2} \\ 1-p_1^{D_2} & p_1^{D_2} \end{bmatrix}, \quad \textbf{(3)}$$

where $p_0^{D_2}$ and $p_1^{D_2}$ are the transition probabilities in the vertical-direction of the source that correspond to the transitions from state s_0 to state s_0 and from state s_1 to state s_1, respectively.

Fig. 1(a) and Fig. 1(b) illustrate the line-by-line scanning defining the transition probabilities of the source in the horizontal-direction and in the vertical-direction, respectively. Thus, there are two sets of transition probabilities required for the exploitation of the 2D source correlation at the receiver.

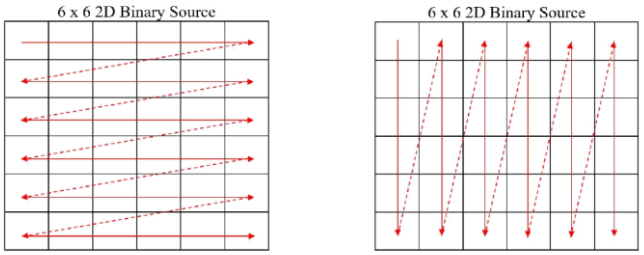

(a) Correlation in horizontal direction: $p_0^{D_1}, p_1^{D_1}$ **(b)** Correlation in vertical direction: $p_0^{D_2}, p_1^{D_2}$

Fig. 1- Line-by-line scanning of 6 x 6 bits 2D source correlation in the (a) horizontal-direction (b) vertical-direction

2.2 The Transmitter Model of the 2D-JSCC-PET1 System

Fig. 2 illustrates the block diagram of the transmitter model for the 2D-JSCC-PET1 system. The 2D sources of u_1 is generated by **S**. The research target is to extend the work of (Mohd Nor et. al., 2018) to evaluate the effectiveness of the 2D-JSCC-PET1 system with the image transmission, thus the same design is used for the transmitter model. Two component encoders for Turbo Single Parity Check Code (TSPCC), C_1 and C_2 are considered. The interleaver, Π_2 is a block interleaver that is used to arrange the source sequence u_1 to a sequence corresponding to the different direction of the source correlation denoted by u_2. A TSPCC uses SPCCs as its component codes and it is known that SPCCs are simple codes that only generate a single parity check bit for any length of information bits. The parity bit sequences, v_1 and v_2 and the source sequence u_1 are multiplexed after the source sequences have been encoded by the component codes. This joined sequence **w** is then rearranged by a random interleaver Π_{in} before passed through an inner encoder C_{in}, which is a rate-1 Recursive Systematic Convolutional Code (RSCC) (Li, Narayanan & Georghiades, 2004). The final encoded sequence **c** is modulated using a BPSK modulator before being transmitted over an Additive White Gaussian Noise (AWGN) channel.

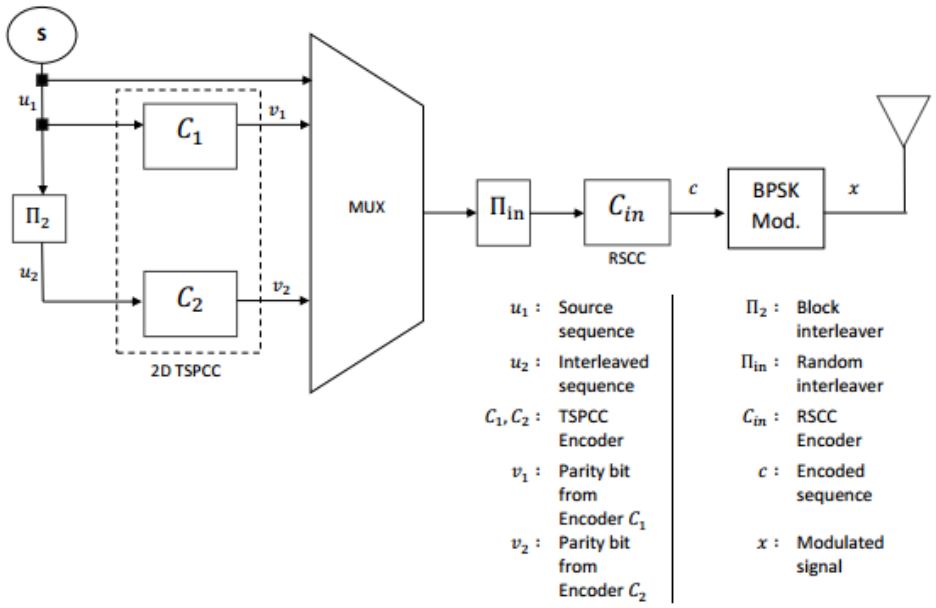

Fig. 2 - The transmitter model of the 2D-JSCC-PET1

2.3 The Receiver Model of the 2D-JSCC-PET1 System

The detailed receiver block diagram of the 2D-JSCC-PET1 system is shown in Fig. 3. The signal from the channel is received and demodulated to generate an output sequence **r.** By using the Bahl-Cocke-Jelinek-Raviv (BCJR) algorithm in C_{in}^{-1}, the sequence **r** is soft decoded via Maximum A Posteriori (MAP) decoding (Bahl, Jelinek & Raviv, 1974). The *a priori* LLR L_a of the coded bit sequence **w** at a time index **t** can be computed as

$$L_a(w_t) = \ln \frac{P(w_t = 1)}{P(w_t = 0)}, \tag{4}$$

where $P(w_t = 1)$ is the probability of w_t has the value equal of 1, while $P(w_t = 0)$ is the probability of w_t holds the value 0. The extrinsic LLR L_e that is generated from C_{in}^{-1} is deinterleaved using Π_{in}^{-1} before fed into C_1^{-1} and C_2^{-1}. The two component decoders correspond to the decoding of the horizontal and vertical direction source sequence. The modified BCJR algorithm is employed to exploit the source correlation throughout the decoding process (Izhar et. al., 2013). Each component decoder yields *a posteriori* LLR and extrinsic LLR outputs. The *a posteriori* LLRs, $L_{app}^1(u_1)$ and $L_{app}^2(u_2)$ are then sent to the Parameter Estimation Technique 1 (PET1) blocks employing the modified BWA to estimate the transition probabilities, $p_0^{D_1}$ and $p_1^{D_1}$ or the horizontal-direction correlation and $p_0^{D_2}$ and $p_1^{D_2}$ for the vertical-direction correlation (Mohd Nor et. al., 2018). The extrinsic LLRs from both activated component decoders that correspond to the source sequence **u** are summed up and multiplexed with all the extrinsic LLRs corresponding to the parity bit sequences. The combined sequence is then interleaved by Π_{in} before feedback to C_{in}^{-1}. The estimated value of the transition probability is updated for a number of iterations to increase the accuracy of the result. After the final iteration, hard decisioning is made to the *a posteriori* LLRs output $L_{app}^2(u_2)$ from C_2^{-1} and then de-interleaved via Π_2^{-1} to generate the decoded bits sequence $\hat{u}$.

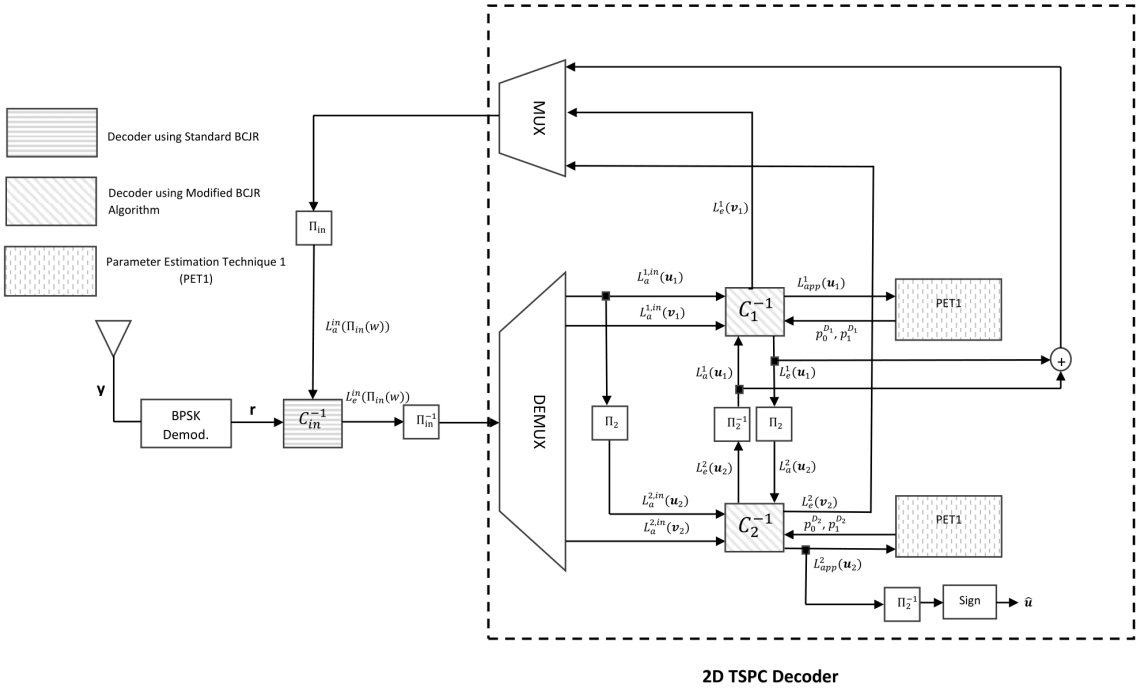

Fig. 3 - The receiver model for the 2D-JSCC-PET1 system

3. Application to Image Transmission

The effectiveness of the proposed 2D-JSCC-PET1 system is demonstrated via image exhibiting strong correlation and image exhibiting weak correlation. The image exhibiting strong correlation known as binary image that consist of only two pixels value that are 0 (refers to black color) and 1 (refers to white color). Each pixel in the binary image contains only 1 bit meanwhile every pixel in the image exhibiting weak correlation or gray-scale image consists of 8 bits. The image is transmitted via the same channel characteristics before decoded using different systems. The considered systems are given as follows:

- The ideal 2D JSCC system The 2D-JSCC-PET1 system
- The 2D-JSCC-PET2 system which is the 2D JSCC system using the parameter estimation technique based on (Zhao, Zhong & Frias, 2006)
- The 2D JSCC system without employing any parameter estimation technique for unknown source correlation knowledge (2D JSCC)
- The non-JSCC system

In this work, Lenna's image is used to represent both image exhibiting strong and weak correlation and the performance is evaluated while exploiting the correlation by two decoders, C_1^{-1} and C_2^{-1} using modified BCJR algorithm. As for the non-JSCC system that does not exploit any source correlation, the standard BCJR algorithm is employed at both decoders, C_1^{-1} and C_2^{-1}. The transition probabilities for both horizontal and vertical directions are calculated using line-by-line scanning prior to its direction. Based on the calculation for the image with strong correlation (binary version of Lenna's image), the transition probabilities are $p_0^{D_1}$ = 0.93 and $p_1^{D_1}$ = 0.93 at the horizontal-direction while at the vertical-direction, the transition probabilities are $p_0^{D_2}$ = 0.95 and $p_1^{D_2}$ = 0.95. For the image with weak correlation (grayscale version of Lenna's image), the transition probabilities are $p_0^{D_1}$ = 0.48 and $p_1^{D_1}$ = 0.46 at the horizontal-direction while at the vertical-direction, the transition probabilities are $p_0^{D_2}$ = 0.72 and $p_1^{D_2}$ = 0.71. For both tests with strong correlation image and weak correlation image, the transition probabilities for the ideal 2D JSCC system were initialized with the actual value as the system is based on the perfect assumption of source correlation knowledge. The transition probabilities values for 2D JSCC systems for unknown source correlation knowledge including the 2D-JSCC-PET1 system were set to 0.5 as the systems are based on unknown source correlation knowledge and need to be estimated. The estimation technique estimates the transition probabilities for both horizontal and vertical directions. The estimated value is utilized for several iterations to yield new estimated value which is expected to get close to the actual transition probabilities.

4. Simulation Results of Image Transmission over AWGN Channel

The image with strong correlation is a binary image of Lenna, as shown in Fig. 4(a) while the image with weak correlation is given by a grayscale image of the Lenna's image, as shown in Fig. 6(a). For the binary image (or the image test 1), dimension of 280 x 280 pixels is used. The simulation settings for the transmission of the image with strong correlation for various systems are given in Table 1.

Table 1 - Simulation Settings for Image Test 1

Parameter	Value
Coding Rate, R_c	0.78
Block Interleaver for Π_2	280 x 280 bits
Random Interleaver for Π_{in}	100,800 bits

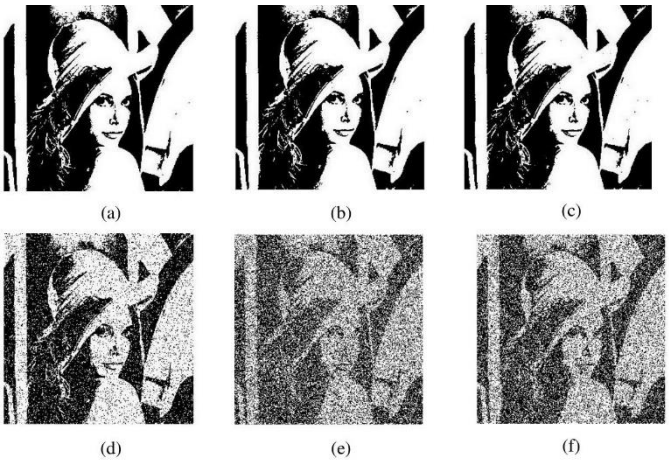

Fig. 4 - Results of image test 1 at E_b/N_0 = -2.1 dB (a) The original transmitted image (b) The ideal 2D JSCC system (c) The 2D-JSCC-PET1 system (d) The 2D-JSCC-PET2 system (e) The JSCC system (f) The non-JSCC system.

4.1 Simulation of an Image Exhibiting Strong Correlation for Different Benchmark Systems

The results of the decoded image test 1 at E_b / N_0 = - 2.1 dB for the 2D-JSCC-PET1 system and other systems are shown in Fig. 4 (b), (c), (d), (e), (f). Table 2 tabulates the pixel-error percentage and PSNR of the resulted images. The best image quality was obtained by the ideal 2D JSCC system, with almost no degradation in quality from the original image (0.01% of pixel error, PSNR of 28.04 dB). Despite the correlation is unknown, the 2D-JSCC-PET1 system shows a slight small difference in image quality compared to the ideal 2D JSCC system with 0.37% of pixel-error percentage and PSNR of 24.30 dB. The 2D-JSCC-PET2 system achieves an SNR improvement of 3.79 dB over the 2D JSCC system and has the pixel-error percentage about 16.52% less than the 2D JSCC system. The non-JSCC system has the lowest image quality with PSNR of 5.09 dB. These results conclude that the 2D-JSCC-PET1 system has advantages over the 2D-JSCC-PET2 system in terms of the image quality while keeping its performance very close to the ideal system.

Fig. 5 illustrates the graph of PSNR (averaged over 100 samples) against E_b / N_0 of the decoded image test 1 from different systems for 10 decoding iterations. The ideal 2D JSCC system has the highest value of PSNR with PSNR of 30 dB achieved at E_b / N_0 = -1.5 dB. The 2D-JSCC-PET1 system has the second highest PSNR value followed by the 2D-JSCC-PET2 system, with PSNR of 30 dB achieved at E_b / N_0 = - 1.14 dB and 1.46 dB, respectively. The system with PSNR of 30 dB obtained at E_b / N_0 = 2.58 dB, succeeded by the JSCC system and the worst performing system is the non-JSCC system achieving PSNR of 30 dB at E_b / N_0 = - 2.61 dB.

Table 2 - Pixel-Error Percentage and PSNR of the Image Results in Fig. 4

System	Pixel-error percentage (%)	PSNR (dB)
Ideal 2D JSCC	0.01	28.04
2D-JSCC-PET1	0.37	24.30
2D-JSCC-PET2	11.02	9.58
2D JSCC	27.52	5.79
Non-JSCC	26.39	5.60

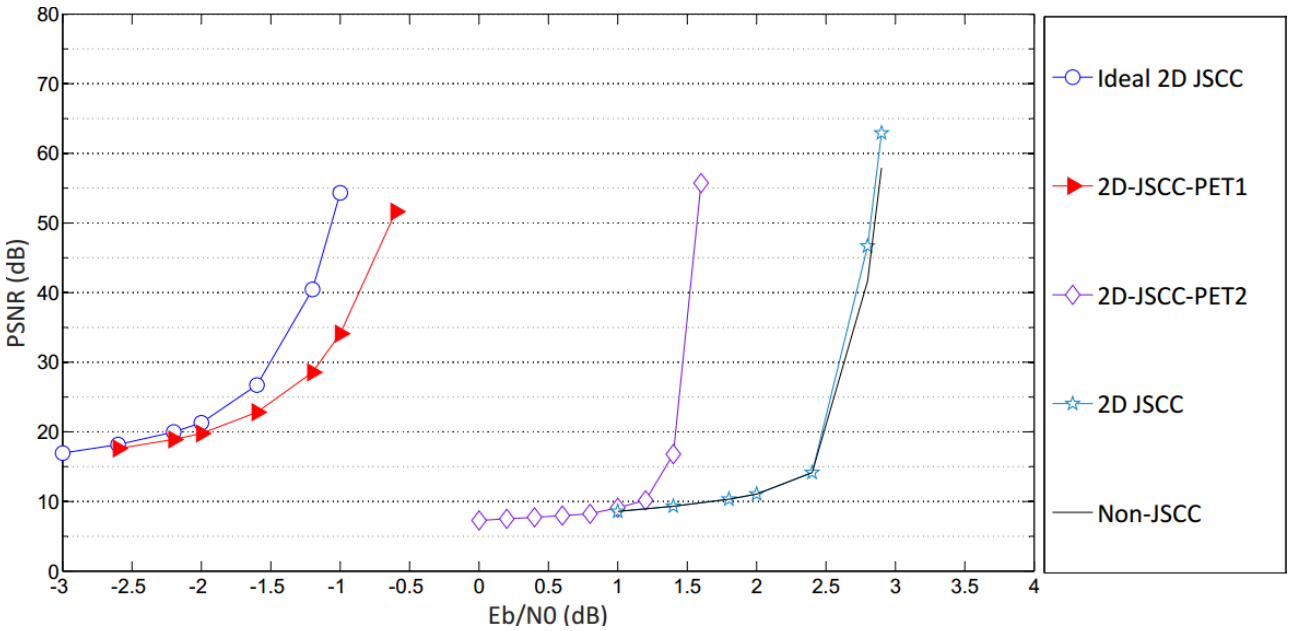

Fig. 5. PSNR performance of test image 1 decoded using various systems after 10 iterations.

4.2 Simulation of an Image Exhibiting Weak Correlation for Different Benchmark Systems

Another image test demonstrating weak source correlation scenario (image test 2) is depicted in Fig. 6(a). The size of the image test 2 is the same with the image test 1 which is 280 x 280 pixels. The only difference is that the grayscale image contains 8 bits per pixel, while the binary image contains one bit per pixel. This image was transformed to a binary matrix of size 280 x 2240 bits before fed to the channel encoder. Identical channel codes and interleaver types with the previous image test were used. The settings used to simulate the gray-scale image transmission is similar to the simulation of an image exhibiting strong correlation as shown in Table 1.

Fig. 6. Results of image test 2 at E_b/N_0 = 2.3 dB (a) The original transmitted image (b) The ideal 2D JSCC system (c) The 2D-JSCC-PET1 system (d) The 2D-JSCC-PET2 system (e) The 2D JSCC system (f) The non-JSCC system.

Fig. 6(b)-(f) depict the results of image test 2 after decoded by different systems. The pixel-error percentage and the the PSNR value for the decoded images in Fig. 6 are tabulated in Table 3. The highest quality of the decoded image is obtained by using the ideal 2D JSCC system with 0.01% of pixel-error percentage from the original image and PSNR of 65.42 dB. The 2D-JSCC-PET1 system resulted in a very small difference in terms of image quality as compared to the ideal 2D JSCC system as there is only 0.061% difference in pixel-error percentage and 11.4 dB less in PSNR. The performance of the 2D-JSCC-PET1 system showed to be better in terms of image quality when compared to the 2D-JSCC-PET2 system as there is 1.39% difference in pixel-error percentage and 13.45 dB greater in PSNR. Both JSCC systems with the parameter estimation techniques achieve significant performance gain compared to the 2D JSCC system. The non-JSCC system has the worst image quality with pixel-error percentage of 10.76% and PSNR of 31.83 dB. This image results demonstrate that even with weak correlation images, the 2D-JSCC-PET1 system can perform very close to the ideal 2D JSCC system and obtain significant performance gain compared to 2D-JSCC-PET2 system, the 2D JSCC system, and the non-JSCC system.

Table 3 - Pixel-Error Percentage and PSNR of the Image Results in Fig. 6

System	Pixel-error percentage (%)	PSNR (dB)
Ideal 2D JSCC	0.01	65.42
2D-JSCC-PET1	0.07	54.02
2D-JSCC-PET2	1.48	40.57
2D JSCC	8.49	32.25
Non-JSCC	10.74	31.83

Fig. 7 illustrates the graph of PSNR versus E_b / N_0 . An over 100 samples were used in the simulation and for each run, 10 iterations were invoked. It can be observed that the PSNR performance of the 2D-JSCC-PET1 system gets very close to the ideal 2D JSCC system where both achieve PSNR of 50 dB at E_b / N_0 of 2.25 dB and 2.21 dB, respectively. On the other hand, the 2D-JSCC-PET2 system outperforms the 2D JSCC system and the non-JSCC system with E_b / N_0 of 2.42 dB at a PSNR of 50 dB. From the results, it can be seen that the performance of the 2D JSCC system is degraded when the system does not employ any parameter estimation technique for unknown source statistics and only achieves PSNR of 50 dB at E_b / N_0 = 2.67 dB. The non-JSCC system has the lowest PSNR performance, with PSNR of 50 dB is achieved at E_b / N_0 = 2.72 dB.

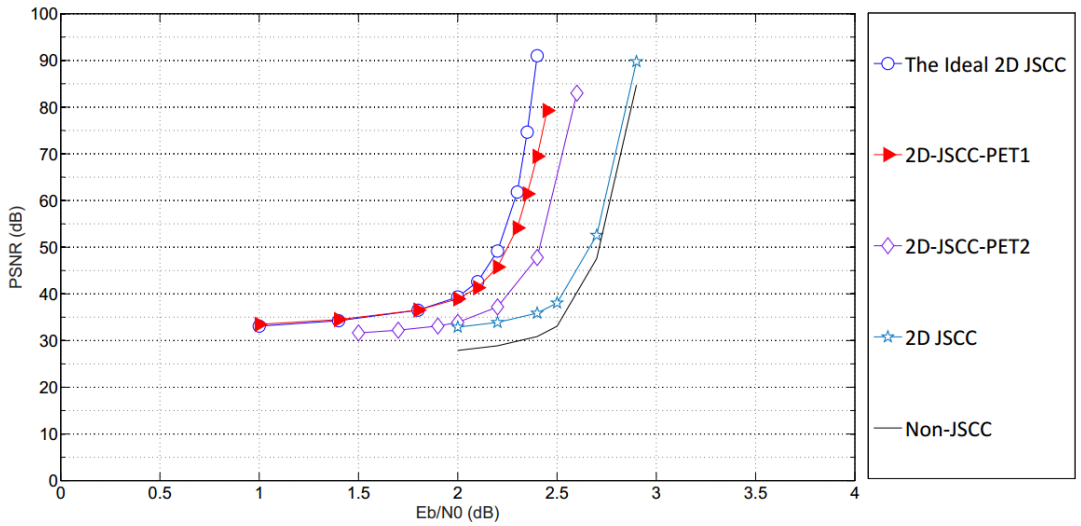

Fig. 7- PSNR performance of image test 2 decoded using various systems after 10 iterations.

The results from the two image tests demonstrate the benefits of the 2D-JSCC-PET1 system. It can be summarized that the performance of the 2D-JSCC-PET1 system becomes very close to the ideal 2D JSCC system in all cases, either with weak or strong source correlation. The 2D-JSCC-PET1 system has better performance than 2D-JSCC-PET2 system indicating that the performance of the system with unknown source statistics can be improved by the accuracy of the parameter estimation algorithm. Both the 2D JSCC systems with parameter estimation show superiority in performance over the similar system without employing any estimation technique.

5. The 2D-JSCC-PET1 system over a Fading Channel

Multi-path propagation or fading effect causes obstruction of free path loss and signal degradation. The received signal's amplitude, phase and angle of arrival fluctuate because of multipath fading. The discrete model of an uncorrelated Rayleigh fading channel can be described by:

$$y_k = h_k x_k + n_k, \quad \textbf{(5)}$$

where k is an integer symbol index, x_k is the symbol amplitude, h_k is a complex-valued channel coefficient and n_k represents AWGN component with zero mean and power spectral density, σ^2. In coherent detection is considered in this work and hence, the receiver is assumed to have sufficient information about the channel impulse response. The transmitted symbols, x_k can be estimated in the form of $\ln P(x_k = m)$ where $m \in \{-1,1\}$ as

$$\ln P(x_k = m) = \frac{|\, y_k - h_k . m \,|}{\sigma^2}. \quad \textbf{(6)}$$

The LLR output from the soft demapper or demodulator, $L_{ch} = (x_k)$ can be formulated as

$$L_{ch}(x_k) = \ln P(x_k = +1) - \ln P(x_k = -1). \quad \textbf{(7)}$$

Since we employ a BPSK modulation scheme, it is worth noting that in Fig. 3, $r_k = L_{ch}(x_k)$.

5.1 BER Performance of 2D-JSCC-PET1 System

BER performance is necessary for the successful design and fine tuning of a digital communications system. Fig. 8 compares the BER performance in fading environment for the 2D-JSCC-PET1 system and the ideal 2D JSCC system with known source statistics (Izhar et. al, 2012) for both the horizontal-direction and the vertical-direction, $p_{D_1} = p_{D_2} = p = 0.9$. Fig. 8 reveals that the 2D source correlation is well exploited at the receiver via the new estimated value obtained from the PET1 module. Both the PET1 blocks are successfully deployed at the receiver to estimate the 2D source correlation. The new estimated value of the transition probabilities in the horizontal-direction and the vertical-direction are fed back to the decoder C_1^{-1} and the decoder C_2^{-1}, respectively to be exploited during channel decoding. About 10 iterations were invoked at the receiver to increase the accuracy of the results and hence, performs closer to the ideal 2D JSCC system.

It is shown in Fig. 8 that the performance of the 2D-JSCC-PET1 system is very close to the ideal 2D JSCC system. The performance gain between the ideal 2D JSCC system and the 2D-JSCC-PET1 system is about the same for $p_{D_1} = p_{D_2} = p = 0.9$. The gain is measured as a difference of E_b / N_0 at the BER level of 10^{-4} between the 2D JSCC systems and the 2D JSCC system without employing any parameter estimation technique for unknown source correlation knowledge. The ideal 2D JSCC system is only slightly better than the 2D-JSCC-PET1 system that shows about 0.88 dB performance difference. However, the ideal system relies on the assumption of perfect source knowledge at the receiver, which may not be suitable practically.

Results in Fig. 8 show that the 2D JSCC system outperforms the 2D-JSCC-PET2 system and the 2D JSCC system with performance difference of 4.23 dB and 6.10 dB, respectively. The performance difference at BER of 10^{-4} for the 2D-JSCC-PET1 system and other benchmark systems are shown in Table 4.

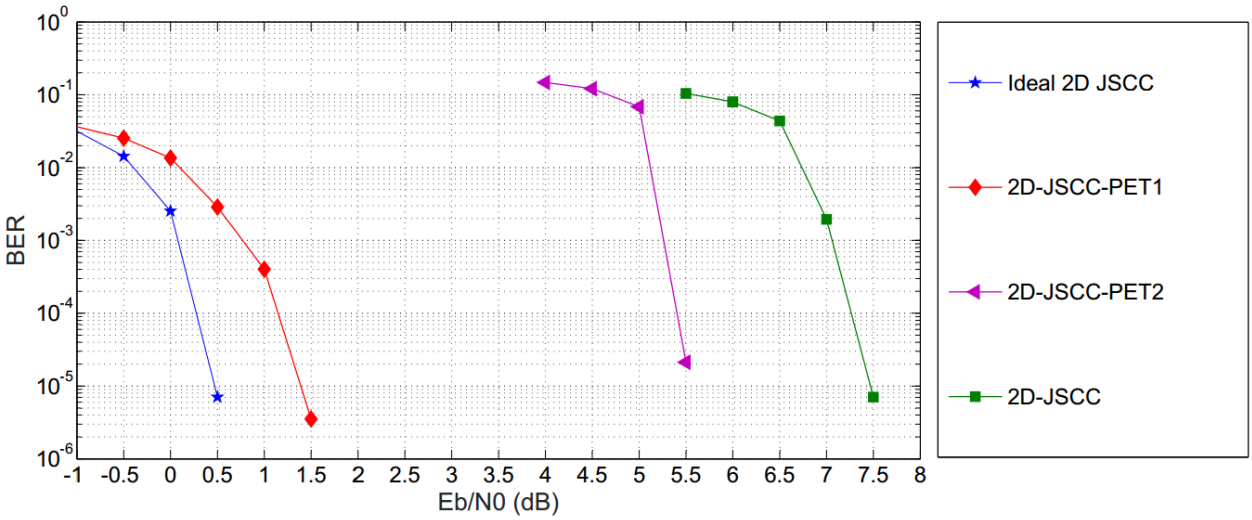

Fig. 8. BER performance of the 2D-JSCC-PET1 system over a Rayleigh fading channel after 10 iterations

Table 4 - The Performance Difference for various systems shown in Fig. 8

System	E_b / N_0 at BER 10^{-4} (dB)	Performance Gain (dB)
Ideal 2D JSCC	0.28	6.98
2D-JSCC-PET1	1.16	6.10
2D-JSCC-PET2	5.39	1.87
2D JSCC	7.26	-

5.2 Simulation of an Image Exhibiting Strong Correlation

The results of the decoded image test 1 over a Rayleigh fading channel at E_b / N_0 =-2.1 dB for the 2D-JSCC-PET1 system and other systems are shown in Fig. 9 (b), (c), (d), (e) and (f). Table 5 tabulates the PSNR of the resulted images. The best image quality was obtained by the ideal 2D JSCC system, with slight degradation in quality from the original image. Despite the correlation is unknown, the 2D-JSCC-PET1 system shows a slight difference in image quality compared to the ideal 2D JSCC system with PSNR of 17.08 dB and outperforms the 2D-JSCC-PET2 system and the 2D JSCC system with PSNR difference of 12.35 dB and 12.40 dB, respectively. The 2D-JSCC-PET2 system achieves almost similar performance as the 2D JSCC system. These results conclude that even in the fading environment, the 2D-JSCC-PET1 system still has advantages over the 2D-JSCC-PET2 system in terms of the image quality while keeping its performance very close to the ideal system.

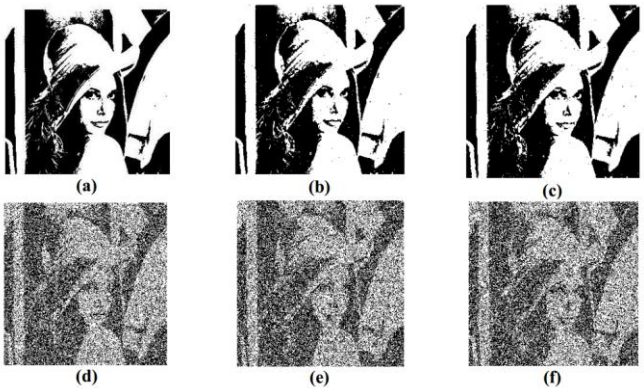

Fig. 9. Results of image test 1 at E_b/N_0 = -2.1 dB (a) The original transmitted image (b) The ideal 2D JSCC system (c) The 2D-JSCC-PET1 system (d) The 2D-JSCC-PET2 system (e) The 2D JSCC system (f) The non-JSCC system.

Table 5 - Pixel-Error Percentage and PSNR of the Image Results in Fig. 9

System	Pixel-error percentage (%)	PSNR (dB)
Ideal 2D JSCC	0.74	17.73
2D-JSCC-PET1	2.06	17.08
2D-JSCC-PET2	33.36	4.73
2D JSCC	33.93	4.68
Non-JSCC	34.01	4.50

5.3 Simulation of an Image Exhibiting Weak Correlation

Another image test demonstrating weak source correlation scenario (image test 2) is depicted in Fig. 10(a). The size of the image test 2 is the same with the image test 1 which is 280 x 280 pixels. The only difference is that the grayscale image contains 8 bits per pixel, while the binary image contains one bit per pixel. This image was transformed to a binary matrix of size 280 x 2240 bits before fed to the channel encoder. Identical channel codes and interleaver types with the previous image test were used.

Fig. 10(b)-(f) depict the results of image test 2 after decoded by different systems for transmission over a Rayleigh fading channel. The PSNR value for the decoded images in Fig. 10 are tabulated in Table 6. The highest quality of the decoded image is obtained by using the ideal 2D JSCC system with PSNR of 31.66 dB. The 2D-JSCC-PET1 system resulted in a very small difference in terms of image quality as compared to the ideal 2D JSCC system as there is 0.43 dB less in PSNR. The performance of the 2D-JSCC-PET1 system indicates better performance in terms of image quality when compared to the 2D-JSCC-PET2 system as there is 1.95 dB greater in PSNR. The 2D-JSCC-PET2 system shows similar performance as the 2D JSCC system. This image results demonstrate that even with weak correlation images over a fading channel, the 2D-JSCC-PET1 system can perform very close to the ideal 2D JSCC system and obtain significant performance gain compared to 2D-JSCC-PET2 system and the 2D JSCC system.

The results from the two image tests demonstrate the benefits of the 2D-JSCC-PET1 system. It can be summarized that even the images transmitted over a fading channel, the performance of the 2D-JSCC-PET1 system can perform well very close to the ideal 2D JSCC system for both cases, weak and strong source correlation

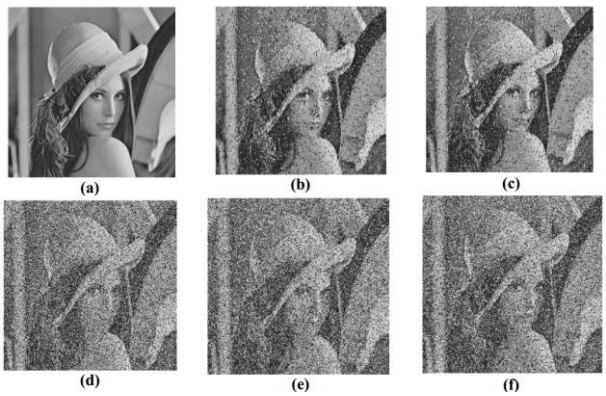

Fig. 10. Results of image test 2 at E_b/N_0 = 2.3 dB (a) The original transmitted image (b) The ideal 2D JSCC system (c) The 2D-JSCC-PET1 system (d) The 2D-JSCC-PET2 system (e) The 2D JSCC system (f) The non-JSCC system.

Table 6 - Pixel-Error Percentage and PSNR of the Image Results in Fig. 10

System	Pixel-error percentage (%)	PSNR (dB)
Ideal 2D JSCC	15.17	31.66
2D-JSCC-PET1	15.52	31.23
2D-JSCC-PET2	21.25	29.29
2D JSCC	21.28	29.28
Non-JSCC	22.78	29.15

Conclusion

This paper investigates the effectiveness of the 2D-JSCC-PET1 system in image transmission over an AWGN channel and extended to be demonstrated in more realistic fading channel. Two image tests have been conducted where the first image is a binary image with strong source correlation and the second image is a grayscale image with weak source correlation. For transmission over the AWGN channel, it has been shown from both image tests that better image quality can be resulted by using the 2D JSCC system as compared to the non-JSCC system. It has been presented in both image tests also that the proposed 2D-JSCC-PET1 system can perform very close to the ideal 2D JSCC system. The difference in PSNR between the 2D-JSCC-PET1 system and the ideal 2D JSCC system is only 5.74 dB at E_b / N_0 = -2.1 dB for the binary image test and 11.4 dB at E_b / N_0 = 2.3 dB for the gray-scale image test. The result tests have also indicated that the 2D-JSCC-PET1 system has better performance than the 2D-JSCC-PET2 system. Explicitly, the 2D-JSCC-PET1 system achieves 14.72 dB higher in PSNR than the 2D-JSCC-PET2 system for the binary image test (at E_b / N_0 = -2.1 dB) and 13.45 dB higher in PSNR than the 2D-JSCC-PET2 system for the gray-scale image test (at E_b / N_0 = 2.3 dB). Meanwhile for the fading channel, it has been revealed from the simulation results that the 2D-JSCC-PET1 system still can achieve performance close to the ideal 2D JSCC system with only 0.88 dB performance difference in E_b / N_0 at a BER of 10^{-4} . For the image simulation over the fading channel, the 2D-JSCC-PET1 system has shown can perform better than the 2D-JSCC-PET2 system and the 2D JSCC system. The performance of the 2D-JSCC-PET1 system is only 0.65 dB and 0.43 dB in PSNR away from the ideal 2D JSCC system for the binary image and grayscale image tests, respectively. The results of the image transmission simulations have successfully demonstrated the effectiveness of the 2D-JSCC-PET1 system with performance very close to the ideal 2D JSCC system over both AWGN and fading channels. The quality of the image can be improved by exploiting higher dimensional source correlation at channel decoder which will be considered in our future work.

Acknowledgement

This work was supported in part by the Malaysian Ministry of Higher Education and in part by the UTM Razak Faculty of Technology and Informatics, Universiti Teknologi Malaysia under HIGDR Grant R.K130000.7740.4J314.

References

[1] Shannon, C. E. (1948). A Mathematical Theory of Communication. The Bell System Technical Journal, 27(3): 379–423. ISSN 0005-8580.
[2] Strunk, W., Jr., & White, E. B. (1979). The elements of style (3rd ed.). New York: MacMillan.
[3] Sayood, K. and Borkenhagen, J. C. (1991). Use of residual redundancy in the design of joint source/channel coders. IEEE Trans. Communications, 39(6): 838–846
[4] Huo, Y., Wang, T., Maunder, R. G. and Hanzo, L. (2013). Iterative source and channel decoding relying on correlation modelling for wireless video transmission. IET Communications, 7(14): 1465–1475. ISSN 1751-8628.
[5] Zhao, Y. and Garcia-Frias, J. (2006). Turbo Compression/Joint Source-channel Coding of Correlated Binary Sources with Hidden Markov Correlation. Signal Process., 86(11): 3115–3122. ISSN 0165-1684.
[6] Belhadj, H., Zaibi, S. and Bouallegue, A. (2008). Iterative joint source-channel decoding with source statistics estimation: application to image transmission. Signal Process. Image Enhance. Multimed. Process. Multimed. Syst. Appl. Ser, 31.
[7] Izhar, M. A. M., Fisal, N., Zhou, X., Anwar, K. and Matsumoto, T. (2012). Utilization of 2-D Markov source correlation using block turbo codes. 7th International Symposium on Turbo Codes and Iterative Information Processing (ISTC). ISSN 2165-4700. 56–60
[8] Izhar, M. A. M., Fisal, N., Zhou, X., Anwar, K. and Matsumoto, T. (2013). Exploitation of 2D binary source correlation using turbo block codes with fine-tuning. EURASIP Journal on Wireless Communications and Networking, 2013(1): 89. ISSN 1687-1499.
[9] Izhar, M. A. M., Kaidi, H. M., Dziyauddin, R. A. and Ahmad, N. (2014). Low complexity technique exploiting 2D source correlation using single parity check codes. IEEE 2nd International Symposium on Telecommunication Technologies (ISTT). 2014. 115–120.
[10] Bi, C. and Liang, J. (2017). Joint Source-Channel Coding of JPEG 2000 Image Transmission Over Two-Way Multi-Relay Networks. IEEE Transactions on Image Processing, 26(7): 3594–3608. ISSN 1057-7149.
[11] Nor, M. I. A. M., Izhar, M. A. M., Ahmad, N., & Kaidi, H. M. (2018). Exploiting 2-Dimensional Source Correlation in Channel Decoding with Parameter Estimation. International Journal of Electrical and Computer Engineering (IJECE), 8(4), 2633-2642.
[12] Hall, E. K. and Wilson, S. G. (1998). Design and analysis of turbo codes on Rayleigh fading channels. IEEE journal on selected areas in communications, 16(2): 160–174.

[13] Gautam, A., Saurabh, K. and Sharma, M. (2014).BER Improvement of BPSK, QPSK and GMSK in Rayleigh fading channel. International Journal of Advanced Engineering Research and Science (IJAERS).
[14] Elfeki, A. M. M. and Dekking, F. M. (2001). A Markov chain model for subsurface characterization: theory and applications. Math. Geol, 33
[15] Li, J., Narayanan, K. R. and Georghiades, C. N. (2004). Product accumulate codes: a class of codes with near-capacity performance and low decoding complexity. IEEE Transactions on Information Theory, 50(1): 31–46.
[16] Bahl, L., Cocke, J., Jelinek, F. and Raviv, J. (1974). Optimal decoding of linear codes for minimizing symbol error rates (corresp.). IEEE Trans. Inf. Theory, 20.
[17] Zhao, Y., Zhong, W. and Garcia-Frias, J. (2006). Transmission of correlated senders over a Rayleigh fading multiple access channel. Signal Processing, 86(11): 3150 – 3159. ISSN 0165-1684. Special Section: Distributed Source Coding.
[18] Xu, H., Hua, K., & Wang, H. (2015). Adaptive FEC coding and cooperative relayed wireless image transmission. Digital Communications and Networks, 1(3), 213-221.
[19] Develi, I., Kabalci, Y., & Basturk, A. (2014). Performance of LDPC coded image transmission over realistic PLC channels for smart grid applications. International Journal of Electrical Power & Energy Systems, 62, 549-555.
[20] Eldin, S. M. S. (2017). Encrypted gray image transmission over OFDM channel for TV cloud computing. International Journal of Speech Technology, 20(3), 431-442.
[21] Lodro, M., Greedy, S., Vukovic, A., Smart, C., & Thomas, D. W. P. (2017). Image transmission using OSTBC-encoded 16-QAM over MIMO time-selective fading channels.
[22] Berceanu, M., Voicu, C., & Halunga, S. (2016). Performance analysis of a large MIMO-CDMA system when image transmission is involved. In Communications (COMM), 2016 International Conference on (pp. 213-216). IEEE.
[23] Aarthi, V., Kannan, S. N., & Ramanshankar, N. (2015, January). Combined source and channel coding for image transmission using enhanced turbo codes in AWGN and Rayleigh fading channel. In Advanced Computing and Communication Systems, 2015 International Conference on (pp. 1-5). IEEE.
[24] Azevedo, R. A., Madeiro, F., Lopes, W. T. A., & Lima, E. A. O. (2016). A quasi random symbol interleaving technique applied to image transmission by noisy channels. IEEE Latin America Transactions, 14(3), 1078-1085.
[25] Majumder, S., & Verma, S. (2015). Iterative decoding of FEC based multiple description codes for image transmission over wireless channel. In Communications (NCC), 2015 Twenty First National Conference on (pp. 1-6). IEEE.